APS(Hadron)/AYNU[2013]

arXiv:1304.6190v1 [hep-ph] 23 Apr 2013

Study the isoscalar mesons $\eta_2(1870)$ and $X(1870)$

Bing Chen* and Ke-Wei Wei
School of Physics and Electrical Engineering, Anyang Normal University, Anyang 455000, China

Ailin Zhang
Department of Physics, Shanghai University, Shanghai 200444, China

(Dated: April 24, 2013)

An isoscalar resonance, $X(1870)$, with a mass $M = 1877.3 \pm 6.3(stat)^{+3.4}_{-7.4}(syst)$MeV and width $\Gamma = 57 \pm 12(stat)^{+19}_{-4}(syst)$MeV was observed by the BesIII Collaboration recently. The mass of $X(1870)$ is compatible with $\eta_2(1870)$ but the decay width is much smaller. In this paper, we analyzed the mass and the two-body strong decay of $\eta_2(1870)$ and $X(1870)$. According to the mass spectra predicted by the Godfrey-Isgur potential model, $X(1870)$ can be candidates of the states $f_1'(2^3P_1)$, $\eta_2'(1^1D_2)$ or $\eta_2(2^1D_2)$. In the Regge trajectories (RTs) framework, $X(1870)$ favors the $\eta'(3^1S_0)$ and $f_1'(2^3P_1)$ assignments. However, the decay properties of $\eta'(3^1S_0)$, $f_1'(2^3P_1)$, $\eta_2'(1^1D_2)$ disagree with the experiments. The two-body strong decay widths indicate that $\eta_2(1870)$ and $X(1870)$ maybe the two different resonant structures. $\eta_2(1870)$ could be assigned to the $\eta_2(2^1D_2)$ quarkonium as the first radical excited state of $\eta_2(1645)$. $X(1870)$ favors a $\eta_H(0^+2^{-+})$ hybrid assignment. Some significant decay modes are suggested to test in future.

PACS numbers: 12.38.Lg, 13.25.Jx

I. INTRODUCTION

Quantum Chromodynamics (QCD) not only allows the $q\bar{q}$ mesons to exist but also enables the exotic states, *e.g.*, glueballs, hybrids, multi-quark states, molecules, ..., to appear in the nature. Although people paid a lot of efforts, no unique experimental signatures of such exotic states have been well established yet [1].

For hybrids, they can carry exotic J^{PC} quantum numbers which are not accessible by the conventional $q\bar{q}$ mesons in the constitute quark model. Experimentally, there are several candidates with exotic J^{PC} [1]. Among them, $\pi_1(1400)$ and $\pi_1(1600)$ maybe the most famous states. Due to its low mass and a single decay mode, $\pi_1(1400)$ looks more like a multi-quark state rather than a hybrid meson. Identification of the $\pi_1(1600)$ as the lightest hybrid seems also premature because the current measurements are not inconsistent with a multi-quark interpretation [2].

Hunting the hybrid mesons with the canonical J^{PC} seems more difficult for the following reasons. Firstly, the predicted mass spectra of hybrid in different models usually overlap the high-excited states of quarkonium. Secondly, both excited quarkonium and hybrid can decay into $L = 0$ and $L = 1$ ("$S + P$") $q\bar{q}$ meson pairs. Finally, the mixing will occur when they carry the same J^{PC}.

A 1^{--} strangeonium-like resonance, $Y(2175)$, which was observed by BaBar Collaboration [3, 4] and confirmed by the BES [5] and Belle [6] Collaborations, was interpreted as a $s\bar{s}g$ candidate [7]. However, the other assignments are still possible, *e.g.*, a 2^3D_1 $s\bar{s}$ state [8], a $s\bar{s}s\bar{s}$ tetraquark state [9, 10], or a threshold effect [11]. The other hybrid candidates, *e.g.*, the 2^{-+} states of $\pi_2(1880)$ and $\eta_2(1870)$, have never been established well.

It is particularly interesting that $\eta_2(1870)$ has been observed in $\gamma\gamma$ reaction [12, 13], radiative J/ψ decays [14] and $p\bar{p}$ annihilation [15, 16]. Its mass determined in these processes are about 1870MeV and the decay width was confirmed to be large (around 200MeV). Now its available mass and width listed by Particle Data Group (PDG) are

$$M = 1842 \pm 8\text{MeV}, \qquad \Gamma = 225 \pm 14\text{MeV}.$$

It should be stressed that the radiative J/ψ decay (Fig.1[A]) and $p\bar{p}$ annihilation are the ideal glueball hunting grounds. But glueball production is suppressed in $\gamma\gamma$ reaction.

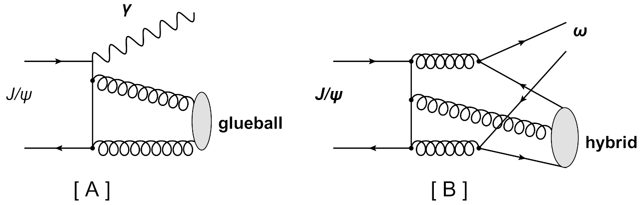

FIG. 1: [A]. A prior production of glueball in the $J/\psi \to \gamma X_G$; [B]. A prior production of hybrid in the $J/\psi \to \omega X_H$.

A new resonant structure of $X(1870)$ was observed by BesIII with a statistical significance of 7.2σ in the channels $J/\psi \to \omega + X(1870) \to \omega\eta\pi^+\pi^-$ recently [17]. Its mass and width were given as

$$M = 1877.3 \pm 6.3^{+3.4}_{-7.4}\text{MeV}, \qquad \Gamma = 57 \pm 12^{+19}_{-4}\text{MeV}.$$

Here the first errors are statistical and the second ones are systematic. The mass of the $X(1870)$ is consistent with $\eta_2(1870)$ but the width is much smaller. By contrast, $X(1870)$ was observed in the hadronic J/ψ decay which is considered "hybrid rich" (Fig.1[B]). If the process, $J/\psi \to \omega{+}X(1870)$, is

---

*Electronic address: chenbing@shu.edu.cn

mainly hadronic, the quantum numbers of $X(1870)$ should be 0^+0^{-+}, 0^+1^{++} or 0^+2^{-+}. The predicted masses for the 0^+0^{-+}, 0^+1^{++} or 0^+2^{-+} hybrids overlap 1.8GeV (see in Table IV) in different models, *e.g.*, the Bag model [18, 19], the flux-tube model [20, 21], the constituent gluon model [22]. Hence, $X(1870)$ becomes a good hybrid candidate.

At present, $\eta_2(1870)$ with $J^{PC} = 2^{-+}$ is listed as a member of 1^1D_2 nonet in PDG with $\eta_2(1645)$, $\pi_2(1670)$ and $K_2(1770)^\dagger$ temporarily [1]. $\eta_2(1870)$ was only observed in the $a_0(980)\pi$, $f_2(1270)\eta$, and $a_2(1320)\pi$ channels, not in the $K\bar{K}\pi$ channel, then it is hard to regard $\eta_2(1870)$ as an excited $\eta'(s\bar{s})$ state unless large $n\bar{n} \leftrightarrow s\bar{s}$ ($n\bar{n} \equiv (u\bar{u} + d\bar{d})/2$) flavor mixing in the $\eta_2(1870)$. However, the near degeneracy of the $\eta_2(1645)$ and $\pi_2(1670)$ argue against this mixing possibility.

$\eta_2(1870)$ has been examined as a quarkonium in the $^3P_0$ model [23]. The authors argued that the interpretation of $\eta_2(1870)$ as a $2^1D_2(n\bar{n})$ state is possible. However, the hybrid interpretation was not excluded there. In addition, the $a_0(980)\pi$ channel which has been observed for $\eta_2(1870)$ wasn't calculated in Ref. [23].

So it is necessary to exhaust the nature of $\eta_2(1870)$ and $X(1870)$ systematically. Some crucial tests to distinguish them are also necessary. In this paper, we will study the masses and strong decays of $X(1870)$ and $\eta_2(1870)$ in detail. The paper is organized as follows. In Sec.II , the masses of $X(1870)$ and $\eta_2(1870)$ are explored in the relativized quark model and the the RTs framework. In Sec.III , the decay properties of these excited isoscalar quarkonium will discussed where the SU(3) favor symmetry has been assumed. Then the two-body strong decay of these states will be explored within the $^3P_0$ model and the flux-tube model. Finally, we will present our conclusions and discussions in Sec.IV.

II. MASS SPECTRUM

Since the masses of $X(1870)$ and $\eta_2(1870)$ are nearly equal, only $X(1870)$ will be discussed in this section for convenience. Obviously, the conclusions are also suitable for $\eta_2(1870)$.

In the Godfrey-Isgur relativized potential model [24], the Hamiltonian consists of the central potential and a kinetic term in a "relativized" form

$$H = \sqrt{\vec{p}_q^2 + m_q^2} + \sqrt{\vec{p}_{\bar{q}}^2 + m_{\bar{q}}^2} + V(r). \qquad (1)$$

The funnel-shaped potentials which includes a color coulomb term at short distances and a linear scalar confining term at large distances are usually incorporated as the zeroth-order potential. The typical funnel-shaped potential was proposed by the Cornell group (Cornell potential) with the form [25]

$$V_{q\bar{q}}(r) = -\frac{4}{3}\frac{\alpha_s}{r} + \sigma r + C. \qquad (2)$$

The strong coupling constant α_s, the string tension σ and the constant C are the model parameters which can be fixed by the well established experimental states. The remaining spin-dependent terms for mass shifts are usually treated as the leading-order perturbations which include the spin-spin contact hyperfine interaction, spin-orbit and tensor interactions and a longer-ranged inverted spin-orbit term. They arise from one gluon exchange (OGE) forces and the assumed Lorentz scalar confinement. The expressions for these terms may be found in Ref [24].

Now, the spin-averaged mass, $\bar{M}_{nl}$, of nL multiplet can be obtained by solving the spinless Salpeter equation which is an approximation of the Bethe-Salpeter equation [26, 27].

$$[\sqrt{\vec{p}_q^2 + m_q^2} + \sqrt{\vec{p}_{\bar{q}}^2 + m_{\bar{q}}^2} + V(r)]\psi(r) = E\psi(r). \qquad (3)$$

Here we employ a variational approach described in Ref. [28] to solve the Eq.(3). This variational approach has been applied in solving the Salpeter equation for $c\bar{s}$ [29], $c\bar{c}$ and $b\bar{b}$ [30] mass spectrum.

In the calculations, the simple harmonic oscillator (SHO) functions are taken as the trial wave functions. It is given by

$$\psi_{nl}(r,\beta) = \beta^{3/2}\sqrt{\frac{2(2n-1)!}{\Gamma(n+l+\frac{1}{2})}}(\beta r)^l e^{-\frac{\beta^2 r^2}{2}} L_{n-1}^{l+1/2}(\beta^2 r^2)$$

in the position space. Here the SHO function scale β is the variational parameter.

By the Fourier transform, the basic SHO radial wave function in the momentum is

$$\psi_{nl}(p,\beta) = \frac{(-1)^n}{\beta^{3/2}}\sqrt{\frac{2(2n-1)!}{\Gamma(n+l+\frac{1}{2})}}(\frac{p}{\beta})^l e^{-\frac{p^2}{2\beta^2}} L_{n-1}^{l+1/2}(\frac{p^2}{\beta^2}).$$

The wave functions of $\psi_{nl}(r,\beta)$ and $\psi_{nl}(p,\beta)$ meet the normalization conditions:

$$\int_0^\infty \psi_{nl}^2(r,\beta)r^2dr = 1; \qquad \int_0^\infty \psi_{nl}^2(p,\beta)p^2dp = 1.$$

In the variational approach, the corresponding $\bar{M}_{nl}$ are given by minimizing the expectation value of H

$$\frac{d}{d\beta}E_{nl}(\beta) = 0. \qquad (4)$$

where

$$E_{nl}(\beta) \equiv \langle H\rangle_{nl} = \langle\psi_{nl}|H|\psi_{nl}\rangle. \qquad (5)$$

When all the parameters of the potential model are known, the values of the harmonic oscillator parameter $\bar{\beta}$ can be fixed directly. With the values of $\bar{\beta}$, all the spin-averaged mass $\bar{M}_{nl}$ will be obtained easily. $\bar{M}_{nl}$ obtained in this way trend to be better for the higher-excited states [31].

It is unreasonable to treat the spin-spin contact hyperfine interaction as a perturbation for the ground states, because the mass splitting between pseudoscalar mesons and vector mesons are much large. Then we consider the contributions of $V_{\vec{s}\cdot\vec{s}}(r)$ for the $1S$ mesons. The following Gaussian-smeared contact hyperfine interaction [32] is taken for convenience,

$$V_{\vec{s}\cdot\vec{s}}(r) = \frac{32\pi\alpha_s}{9m_q^2}(\frac{\kappa}{\sqrt{\pi}})^3 e^{-\kappa^2 r^2}\vec{S}_q \cdot \vec{S}_{\bar{q}}. \qquad (6)$$

In this work, we choose the model parameters as follows: $m_u = m_d = 0.220$ GeV, $m_s = 0.428$ GeV, $\alpha_s = 0.6$, $\sigma = 0.143$ GeV^2, $\kappa = 0.37$ GeV, and $C = -0.37$ GeV. A smaller σ was obtained by the relation between the slope of the Regge trajectory for the Salpeter equation α' and the slope α'_{st} in the string picture [33]. This smaller value for σ is taken here rather than the value in Ref. [24]. The Gaussian smearing parameter κ seems a little smaller than that in Ref. [24]. However, the κ is usually fitted by the hyperfine splitting of low-excited nS states in the literatures with a certain arbitrariness.

The values of $\overline{M}_{nL}$ and $\bar{\beta}$ for the states $2S$, $3S$, $4S$, $1P$, $2P$, $3P$, $1D$, $2D$, $3D$, $1F$, $2F$, $1G$ and $1H$ are listed in TableI. The experimental masses for the relative mesons are taken from PDG [1].

States	$\overline{M}_{nl}(n\bar{n})$	$\bar{\beta}$	$\overline{M}_{nl}$ [1]	$\overline{M}_{nl}(s\bar{s})$	$\bar{\beta}$	$\overline{M}_{nl}$ [1]
1S	-	0.44 0.34	-	-	0.42 0.39	-
2S	1.399	0.310	1.389	1.631	0.330	1.629
3S	1.859	0.295		$\underline{2.069}$	0.310	
4S	2.240	0.290		2.436	0.300	
1P	1.252	0.310	1.257	1.460	0.340	1.478
2P	1.711	0.294		$\underline{1.926}$	0.315	
3P	2.110	0.290		2.308	0.300	
1D	1.661	0.280	1.672	$\underline{1.883}$	0.300	
2D	$\underline{2.067}$	0.276		2.272	0.292	
3D	2.417	0.275		2.609	0.288	
1F	1.924	0.277		2.128	0.295	
2F	2.287	0.275		2.478	0.290	
1G	2.161	0.275		2.350	0.292	
1H	2.377	0.273		2.554	0.287	

TABLE I: The spin-averaged mass (unit: GeV) and the harmonic oscillator parameter $\bar{\beta}$ (unit: GeV^{-1}) of the states $2S$, $3S$, $4S$, $1P$, $2P$, $3P$, $1D$, $2D$, $3D$, $1F$, $2F$, $1G$ and $1H$.

Obviously, the spin-averaged masses of the $2S$, $1P$, $1D$ $n\bar{n}$ and $1P$, $2S$ $s\bar{s}$ mesons are consistent with the experimental data. Indeed, the predicted masses of higher excited states here are also reasonable, *e.g.*, $a_4(2040)$ and $f_4(2050)$ are very possible the $F-$wave $n\bar{n}$ isovector and isoscalar mesons with the mass 1996^{+10}_{-9}MeV, 2018±11MeV [1]. The predicted spin-averaged mass of $1F$ is compatible with experiments. The presented $\overline{M}_{nL}$ in Table I are also overall in good agreement with the expectations from Ref. [34].

In the calculations, we ignored the Coulomb interaction for $1D$, $2D$, $1F$, $1G$ and $1H$ states. In this way, $\overline{M}_{nl}$ for these states increase about 100MeV. As shown in Ref. [34, 35], the masses for higher excited states with $\sigma = 0.143$GeV^2 and $\alpha_s = 0$ are closer to experimental data than the results given in Ref. [24].

The trend that a higher excited state corresponds to a smaller $\bar{\beta}$ coincides with Ref. [36–38]. It needs to mention that the strong decay amplitudes given by the $^3P_0$ model often contain the nodal-type Gaussian form factors which can lead to a dynamic suppression for some channels. Then the values of β are important when one use the $^3P_0$ model to exact the decay width for the higher excited mesons.

The masses of $\eta'(3^1S_0)$, $f'_1(2^3P_1)$, $\eta'_2(1^1D_2)$ and $\eta_2(2^1D_2)$ are usually within 1.9 ∼ 2.1GeV in various quark potential models (see in Table II). The predicted regions are compatible with the spin-averaged masses of $3S(s\bar{s})$, $2P(s\bar{s})$, $1D(s\bar{s})$ and $2D(n\bar{n})$ presented in Table I. Due to the uncertainty of the potential models, absolute deviation from experimental data are usually about 100∼150MeV for the higher excited states. Comparing with these predicted masses, $X(1870)$ disfavor the $\eta'(3^1S_0)$ assignment for its low mass. But the possibilities of $f'_1(2^3P_1)$, $\eta'_2(1^1D_2)$ and $\eta_2(2^1D_2)$ still exist.

States	$\eta'(3^1S_0)$	$f'_1(2^3P_1)$	$\eta'_2(1^1D_2)$	$\eta_2(2^1D_2)$
Ref. [24]	–	2030	1890	$2130^{\dagger}$
Ref. [39]	2085	2016	1909	1960
Ref. [40]	2099	1988	1851	–

TABLE II: The masses predicted for $3^1S_0(\eta')$, $2^3P_1(\eta')$, $1^1D_2(\eta')$ and $2^1D_2(\eta)$ in Ref. [24, 39, 40].

Regge trajectories (RTs) is another useful tool for studying the mass spectrum of mesons. The linearity and parallel of RTs in heavy-light and heavy-heavy mesons is still in debate. In Ref. [41], the authors fitted the RTs for all light-quark meson states listed in the PDG tables. A global description was constructed as

$$M^2 = 1.38(4)n + 1.12(4)J - 1.25(4). \tag{7}$$

$h_1(1380)$, $f_1(1420)$ and $\eta'(1475)$ have been established as the 1^1P_1, 1^3P_1 and 2^1S_0 $s\bar{s}$ mesons in PDG [1]. With the mass difference between the mass squared of $X(1870)$ and these states (Table III), $X(1870)$ could be assigned for the $\eta'(3^1S_0)$ and $f'_1(2^1P_1)$. The mass of $X(1870)$ is too large for the $\eta'_2(1^1D_2)$ state in the RTs. $\eta_2(1645)$ has been assigned as the 1^1D_2 $n\bar{n}$ meson [1]. Since $M^2(X(1870)) - M^2(\eta_2(1640)) \approx 0.91$ which is much smaller than 1.38(4), $X(1870)$ can't be accepted as the 2^1D_2 $n\bar{n}$ state for its low mass.

The mass of $X(1870)$ in the RTs			
$\eta'(3^1S_0)$	$f'_1(2^3P_1)$	$\eta'_2(1^1D_2)$	$\eta_2(2^1D_2)$
$\eta'(1475)$	$f_1(1420)$	$h_1(1380)$	$\eta_2(1645)$
1.34	1.38	1.60	0.91

TABLE III: $X(1870)$ calculated in RTs for different states are shown.

As mentioned in the Introduction, $X(1870)$ is also a good hybrid candidate since its mass overlaps the predictions given by different models (Table IV).

States	$\eta_H(0^+0^{-+})$	$f_H(0^+1^{++})$	$\eta_H(0^+2^{-+})$
Bag [18, 19]	1.3	heavier	1.9
Flux tube [20, 21]	1.7∼1.9	1.7∼1.9	1.7∼1.9
Constituent gluon [22]	1.8∼2.2	1.3∼1.8	1.8∼2.2

TABLE IV: The masses predicted for $\eta_H(0^+0^{-+})$ $f_H(0^+1^{++})$ and $\eta_H(0^+2^{-+})$ hybrid states in Ref. [18–22].

In summary, the $X(1870)$ could be a $f_1'(2^3P_1)$, $\eta_2'(1^1D_2)$ or $\eta_2(2^1D_2)$ meson in the Godfrey-Isgur quark potential model with a reasonable uncertainty. In the RTs, $X(1870)$ favors the $\eta(3^1S_0)$ and $f_1'(2^3P_1)$ assignments. $X(1870)$ is also a good hybrid state candidate. The investigations of the strong decay properties will be more helpful to shed light on the underlying structure of this state.

III. THE STRONG DECAY

A. The final mesons include the scalar mesons below 1 GeV

Despite many theoretical efforts, the scalar nonet of light mesons has never well-established. The lowest-lying scalar mesons including $\sigma(500)$ (or $f_0(600)$), $\kappa(800)$, $a_0(980)$ and $f_0(980)$ are difficult to be described as $q\bar{q}$ states, *e.g.*, $a_0(980)$ is associated with nonstrange quarks in the $q\bar{q}$ scheme. If this is true, its high mass and decay properties are difficult to be understood simultaneously. So interpretations as exotic states were triggered, *i.e.*, as two clusters of two quarks and two antiquarks [42], particular quasimolecular states [43], and uncorrelated four quark states $qq\overline{qq}$ [44] have been proposed.

Though the structures of these scalar mesons below 1 GeV are still in dispute, the viewpoint that these scalar mesons can constitute a complete nonet states has been reached in most literatures (as illustrated in Fig.2). In the following, we will denote this nonet as " $\mathcal{S}$ " multiplet for convenience.

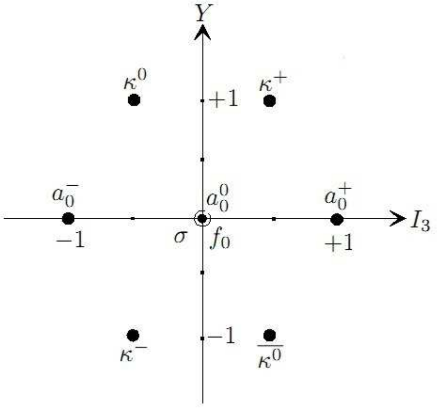

FIG. 2: The $\mathcal{S}$ nenet below 1 GeV shown in $Y - I_3$ plane.

Due to the unclear mechanism, it seems much difficult to study the decay processes where the final mesons includes a $\mathcal{S}$ member. In Ref. [45, 46], $a_0(980)$, $\sigma(500)$ and $f_0(980)$ were treated as 1^3P_0 $q\bar{q}$ mesons approximately. In Ref [23, 47], the decay channels including the $\mathcal{S}$ meson have been ignored. However, this kind of decay channel maybe predominant for some mesons. For example, the observations indicate that $X(1870)$ primarily decay via the $a_0(980)\pi$ channel [17].

In what follows we will obtain some useful information about this kind of decay mode where the SU(3) flavor symmetry shall be invoked. We will show that $a_0(980)\pi$, $\sigma_0\eta$ and $f_0\eta$ are the main decay channels for the isoscalar $n\bar{n}$ and the $n\bar{n}g$ mesons when they decay primarily through " $\mathcal{S}$ + P" mesons, where the sign "P" denotes a light pseudoscalar meson. This explains why $X(1870)$ has been first observed in the $\eta\pi^+\pi^-$ channel.

We noticed that the $\mathcal{S}$ nonet could be interpreted like the $q\bar{q}$ nonet in the diquark-antidiquark scenario. In Wilczek and Jaffe's terminology [48, 49], the $\mathcal{S}$ mesons consist of a "good" diquark and a "good" antidiquark. When u, d quarks forms a "good" diquark, it means that the two light quarks could be treated as a quasiparticle in color $\bar{3}$, flavor $\bar{3}$ and the spin singlet, which denotes as $[ud]$.

In the diquark-antidiquark limit, the parity of a tetraquark is determined by $P = (-1)^{L_{12-34}}$ [50] where the L_{12-34} refer to the relative angular momentum between two clusters. Thus the $\mathcal{S}$ mesons are the lightest tetraquark states in the diquark-antidiquark model with $L_{12-34} = 0$. The $\mathcal{S}$ nonet in the full set of flavor representations is

$$(3 \otimes 3)_{\bar{3}} \otimes (\bar{3} \otimes \bar{3})_3 = 8 \oplus 1$$

Because the SU(3) flavor symmetry is not exact, two physical isoscalar mesons, σ_0 and f_0, are usually the mixing states of the $|8\rangle_{I=0}$ and $|1\rangle_{I=0}$ states [42],

$$\begin{pmatrix} f_0 \\ \sigma_0 \end{pmatrix} = \begin{pmatrix} \cos\vartheta & \sin\vartheta \\ -\sin\vartheta & \cos\vartheta \end{pmatrix} \begin{pmatrix} |8\rangle_{I=0} \\ |1\rangle_{I=0} \end{pmatrix} \tag{8}$$

When the mixing angle ϑ equals the so-called ideal mixing angle, *i.e.*, $\vartheta = 54.74°$, the composition of the $\sigma(500)$ and $f_0(980)$ are

$$\begin{pmatrix} f_0 \\ \sigma_0 \end{pmatrix} = \begin{pmatrix} |\frac{1}{\sqrt{2}}([su][\overline{su}] + [sd][\overline{sd}])\rangle \\ |[ud][\overline{ud}]\rangle \end{pmatrix}.$$

The deviation from the ideal mixing angle of the the $\sigma(500)$ and $f_0(980)$ is small [42]. In the following calculations, we will treat them in the ideal mixing scheme.

Under the SU(3) flavor assumption, all the members of the octet have the same basic coupling constant in one type of reaction, while the singlet member have a different coupling constant. Particularly, when a quarkonium decays into $\mathcal{S}$ and $q\bar{q}$ mesons, there are five independent coupling constants, *i.e.*, g_{A88} g_{A81}, g_{A18}, g_{B88} and g_{B11}, corresponding to five different channels

$$\begin{cases} |\,8\rangle_{q\bar{q}} \to |\,8\rangle_{\mathcal{S}} \otimes |\,8\rangle_{q\bar{q}} : & g_{A88} \\ |\,8\rangle_{q\bar{q}} \to |\,8\rangle_{\mathcal{S}} \otimes |\,1\rangle_{q\bar{q}} : & g_{A81} \\ |\,8\rangle_{q\bar{q}} \to |\,1\rangle_{\mathcal{S}} \otimes |\,8\rangle_{q\bar{q}} : & g_{A18} \\ |\,1\rangle_{q\bar{q}} \to |\,8\rangle_{\mathcal{S}} \otimes |\,8\rangle_{q\bar{q}} : & g_{B88} \\ |\,1\rangle_{q\bar{q}} \to |\,1\rangle_{\mathcal{S}} \otimes |\,1\rangle_{q\bar{q}} : & g_{B11} \end{cases}$$

In order to determine the relations between these coupling constants, we shall assume the process that a $q\bar{q}$ meson decays into a $\mathcal{S}$ and another $q\bar{q}$ mesons obeys the OZI (Okubo-Zweig-Iizuka) rule, *i.e.*, the two quarks in the mother meson go into two daughter mesons respectively. Therefore, there are four forbidden processes, $X(\frac{1}{\sqrt{2}}(u\bar{u} - d\bar{d})) \nrightarrow a_0 + s\bar{s}$, $X(\frac{1}{\sqrt{2}}(u\bar{u} +$

$d\bar{d})) \nrightarrow \sigma_0+s\bar{s}$, $X(s\bar{s}) \nrightarrow f_0+\frac{1}{\sqrt{2}}(u\bar{u}+d\bar{d})$ and $X(s\bar{s}) \nrightarrow \sigma_0+s\bar{s}$. With the help of the SU(3) Clebsch−Gordon coefficients [51], the ratios between the five coupling constants are extracted by the four forbidden processes as

$$g_{A81} : g_{A18} : g_{B88} : g_{B11} : g_{A88} \approx 1.41 : -2.05 : -2.89 : -2.05 : 1 \tag{9}$$

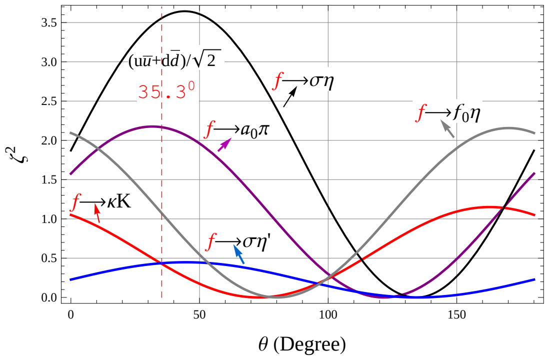

FIG. 3: The coefficients ζ^2 of f versus the mixing angle θ.

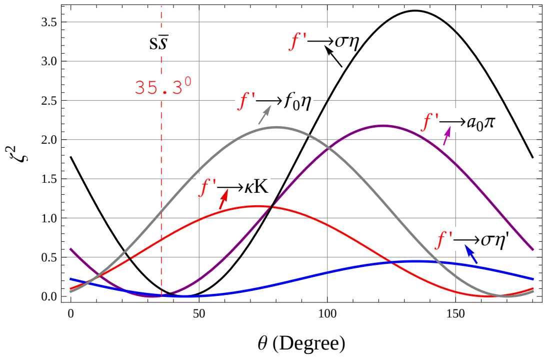

FIG. 4: The coefficients ζ^2 of f' versus the mixing angle θ.

It is well known that the physical states, $\eta(548)$ and $\eta'(958)$ are the mixture of the SU(3) flavor octet and singlet. They are written in terms of a mixing angle, θ_p, as follows

$$\begin{pmatrix} \eta(548) \\ \eta'(958) \end{pmatrix} = \begin{pmatrix} \cos\theta_p & -\sin\theta_p \\ \sin\theta_p & \cos\theta_p \end{pmatrix} \begin{pmatrix} |8\rangle_{I=0} \\ |1\rangle_{I=0} \end{pmatrix} \tag{10}$$

The mixing angle θ_p has been measured by various means. However, there is still uncertainty for θ_p. An excellent fit to the tensor meson decay widths was performed under the SU(3) symmetry, and $\theta_p \simeq -17^o$ was obtained [52]. In our calculation, we take θ_p as -17^o. The excitation of $n\bar{n}$ and $s\bar{s}$ are denoted as

$$\begin{pmatrix} f(n\bar{n}) \\ f'(s\bar{s}) \end{pmatrix} = \begin{pmatrix} \cos\theta & \sin\theta \\ -\sin\theta & \cos\theta \end{pmatrix} \begin{pmatrix} |1\rangle_{I=0} \\ |8\rangle_{I=0} \end{pmatrix} \tag{11}$$

In this scheme, the ideal mixing occurs for the choice of $\theta = 35.3^o$. When f and f' decay into a $\mathcal{S}$ and pseudoscalar mesons, the relations of decay amplitudes are governed by the coefficients ζ^2 which are model-independent. With the coupling constants in hand, the coefficients ζ^2 of f and f' versus the mixing angle θ are shown in the Fig.3 and Fig.4. When f and f' occurs in the ideal mixing, the values of ζ^2 are presented in Table V where the mixing of $\eta(548)$ and $\eta'(958)$ has been considered.

Decay channels	$a_0\pi$	$\sigma\eta$	κK	$f_0\eta$	$\sigma\eta'$
$\zeta^2[n\bar{n}]$	2.17	3.56	0.47	1.07	0.44
$\zeta^2[s\bar{s}]$	0.00	0.00	0.72	1.08	0.00

TABLE V: .The coefficients ζ^2 of f and f' in the ideal mixing.

It is sure that the ζ^2 are zero for the processes, $f' \to a_0\pi$, $f' \to \sigma\eta$ and $f' \to \sigma\eta'$, since they are OZI-forbidden. ζ^2 of $f' \to f_0\eta'$ hasn't been considered in Table V because X(1870) lies below the threshold of $f_0\eta'$.

As illustrated in the Fig.3 and Fig.4, the primary decay channels for $f'(s\bar{s})$ are $f_0\eta$ and κK when the mixing angle of $f(n\bar{n})$ and $f'(s\bar{s})$ is not large. Indeed, only the ground 0^{-+} and the 0^{++} isoscalar mesons are not close to ideally mixed. Since $X(1870)$ primarily decay via the $a_0(980)\pi$ channel, it should be a $(u\bar{u}+d\bar{d})/\sqrt{2}$ predominant meson.

What's more, $\eta_2(1870)$ was observed in the $a_0(980)\pi$, $f_2(1270)\eta$, and $a_2(1320)\pi$ channels, not in the $KK\pi$ channel. Therefore, the only possible assignment for $\eta_2(1870)$ and $X(1870)$ as a canonical quarkonium is the $\eta_2(2^1D_2)$ state. If $\eta_2(1870)$ occupies this state, $X(1870)$ shall be a hybrid meson for its narrow width [53]. Next, we will explore the two-body strong decay of them to pin down this possibility.

B. The strong decays of $\eta_2(1870)$ and $X(1870)$

Firstly, we employ the quark-pair creation model, also known as the $^3P_0$ model [54, 55], to compute the two-body strong decay of $X(1870)$ as the $\eta_2(2^1D_2)$ $q\bar{q}$ meson. This model has achieved great success in calculating the two-body strong decay of different hadrons (see Ref. [56] and references therein).

In the nonrelativistic limit, the transition operator $\hat{\mathcal{T}}$ of the $^3P_0$ model is depicted as

$$\hat{\mathcal{T}} = -3\gamma\sum_{m}\langle 1,m;1,-m|0,0\rangle\iint d^3\vec{k}_3 d^3\vec{k}_4\delta^3(\vec{k}_3+\vec{k}_4)\mathcal{Y}_1^m(\frac{\vec{k}_3-\vec{k}_4}{2})\omega_0^{(3,4)}\varphi_0^{(3,4)}\chi_{1,-m}^{(3,4)}d_{3i}^\dagger(\vec{k}_3)d_{4j}^\dagger(\vec{k}_4) \tag{12}$$

Here, $\omega_0^{(3,4)}$ and $\varphi_0^{(3,4)}$ are the color and flavor wave functions of the $q_3\bar{q}_4$ pair created from vacuum. Thus, $\omega_0^{(3,4)} = (R\bar{R}+G\bar{G}+B\bar{B})/\sqrt{3}$, $\varphi_0^{(3,4)} = (u\bar{u}+d\bar{d}+s\bar{s})/\sqrt{3}$ are color and flavor singlets. The pair is also assumed to carry the quantum numbers of 0^{++}, suggesting that they are in a $^3P_0$ state. Then $\chi_{1,-m}^{(3,4)}$ represents the pair production in a spin triplet state. The solid harmonic polynomial $\mathcal{Y}_1^m(\vec{k}) \equiv |\vec{k}|\mathcal{Y}_1^m(\theta_k,\phi_k)$ reflects the momentum-space distribution of the $q_3\bar{q}_4$.

γ is a dimensionless constant which denotes the strength of the quark-antiquark pair created from vacuum. It is usually extracted by fitting the measured partial decay widths. More details of γ will be discussed later. The helicity amplitude $\mathcal{M}^{M_{J_A},M_{J_B},M_{J_C}}(p)$ of $A \to B+C$ is given by

$$\langle BC|\hat{\mathcal{T}}|A\rangle = \delta^3(\vec{P}_A-\vec{P}_B-\vec{P}_C)\mathcal{M}^{M_{J_A},M_{J_B},M_{J_C}}(p), \tag{13}$$

where p represents the momentum of the outgoing meson in the rest frame of the meson A. When the mock state [57] is adopted to describe the spatial wave function of a meson, the helicity amplitude $\mathcal{M}^{M_{J_A},M_{J_B},M_{J_C}}(p)$ can be constructed in the $L-S$ basis easily [55]. The mock state for A meson is

$$\begin{aligned}&|A(n_A{}^{2S_A+1}L_A^{J_AM_{J_A}}(\vec{P}_A))\rangle\\ &\quad\equiv\sqrt{2E_A}\sum_{M_{L_A}M_{S_A}}\langle L_AM_{L_A}S_AM_{S_A}|J_AM_{J_A}\rangle\omega_A^{12}\phi_A^{12}\chi_{S_AM_{S_A}}^{12}\\ &\quad\times\int d\vec{P}_A\psi_{n_A}^{L_AM_{L_A}}(\vec{k}_1,\vec{k}_2)|q_1(\vec{k}_1)q_2(\vec{k}_2)\rangle.\end{aligned} \tag{14}$$

To obtain the analytical amplitudes, the SHO wave functions are usually employed for $\psi_{n_A}^{L_AM_{L_A}}(\vec{k}_1,\vec{k}_2)$. For comparison with experiments, one obtains the partial decay width $\mathcal{M}^{JL}(p)$ via the Jacob-Wick formula [58]

$$\begin{aligned}\mathcal{M}_{LS}(p) =&\frac{\sqrt{2L+1}}{2J_A+1}\sum_{M_{J_B},M_{J_C}}\langle L0JM_{J_A}|J_AM_{J_A}\rangle\\ &\times\langle J_B,M_{J_B}J_C,M_{J_C}|JM_{J_A}\rangle\mathcal{M}^{M_{J_A},M_{J_B},M_{J_C}}(p).\end{aligned} \tag{15}$$

Finally, the decay width $\Gamma(A \to BC)$ is derived analytically in terms of the partial wave amplitudes

$$\Gamma(A \to BC) = 2\pi\frac{E_BE_C}{M_A}p\sum_{LS}|\mathcal{M}_{LS}(p)|^2. \tag{16}$$

More technical details of the $^3P_0$ model can be found in Ref. [55]. The inherent uncertainties of the $^3P_0$ decay model itself have been discussed in the Ref. [59–61].

The nature of γ has been investigated in several works. Firstly, the relations of the $^3P_0$ model to "microscopic" QCD decay mechanisms have been studied in Ref [62]. There, the authors found that the constant γ corresponds approximately to the dimensionless combination, $\sigma/m_q\beta$, where β means the meson wave function scale, m_q is the mass of produced quark and σ is the string tension. Secondly, the momentum dependent manner of γ has been studied in Ref [61]. It was found that γ is dependent on the relative momentum of the created $q\bar{q}$ pair, and the form of $\gamma(k) = A+B\exp(-Ck^2)$ with $k = |\vec{k}_3-\vec{k}_4|$ was suggested. Thirdly, J.Segovia, *et al.*, proposed that γ is a function of the reduced mass of quark-antiquark pair of the decaying meson [63].

Based on the first and third points above, γ will depend on the flavors of both the decaying meson and produced pairs. In the following, we treat the γ as a free parameter and fix it by the 8 well-measured partial decay widths which are listed in TableVI. The $\mathcal{M}_{LS}$ amplitudes of these decay channels are presented explicitly in the Appendix A.

Decay channels	p (GeV)	$\gamma(10^3)$	γ[61]	Decay channels	p (GeV)	$\gamma(10^3)$	γ[61]
$\rho \to \pi\pi$	0.362	17.8	9.18	$f_1' \to K^*\bar{K}$	0.158	4.9	-
$a_2 \to \eta\pi$	0.535	11.5	-	$f_2 \to K\bar{K}$	0.401	2.9	6.11
$f_2 \to \pi\pi$	0.622	7.8	7.13	$a_2 \to K\bar{K}$	0.434	2.3	3.91
$\rho_3 \to \pi\pi$	0.833	4.2	-	$f_2' \to K\bar{K}$	0.579	2.0	5.66

TABLE VI: . Values of γ in different channels and comparison with the results given by Ref.[61]. $\rho(770)$, $a_2(1320)$, $f_1'(1420)$, $f_2(1270)$, $f_2'(1525)$ and $\rho_3(1690)$ have been studied.

These 8 decay channels are divided into two groups: one is $n\bar{n} \to n\bar{s}+n\bar{s}$, the other includes $s\bar{s} \to n\bar{s}+s\bar{n}$ and $n\bar{n} \to n\bar{s}+s\bar{n}$. The values of γ here are a little different from these given in Ref.[61] where an $AL1$ potential was selected to determine the meson wave functions. Of course, the meson wave function given by different potentials will influence the values of γ.

It is clear in Table VI that γ decrease when p increase. In addition, our calculation indicates that γ depend on flavors of both the decaying meson and the produced quark pairs. For example, values of γ fixed by $a_2 \to K\bar{K}$ and $f_2' \to K\bar{K}$ are roughly equal.

In the following calculations, we assume that the values of γ corresponding to the processes of $s\bar{s} \to n\bar{s}+s\bar{n}$ and $n\bar{n} \to n\bar{s}+s\bar{n}$ are determined by one function. Similarly, we take the function, $\gamma(p) = A+B\exp(-Cp^2)$, for the creation vertex. With the four decay channels listed in fifth column of Table VI, we fix the function as $\gamma(p) = 1.8+4\exp(-10p^2)$. For the processes of $n\bar{n} \to n\bar{n}+n\bar{n}$ (the first column of Table VI), we fix the creation vertex function as $\gamma(p) = 3.0 + 25\exp(-4p^2)$. The dependence of γ on the momentum p are plotted in the Fig. 5. Obviously the functions can describe the dependence of γ and p well. The functions of creation vertex given here need to be tested further.

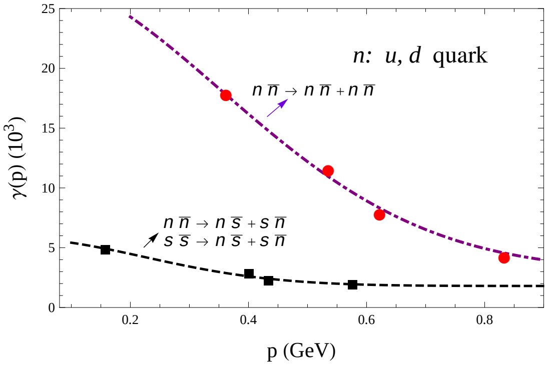

FIG. 5: The functions of $\gamma(p) = A + B\exp(-Cp^2)$ in different decay processes. The symbols of red "●" and black "■" denote γ values determined by the experimental data.

Since we neglected the mass splitting within the isospin multiplet, the partial width into the specific charge channel should be multiplied by the flavor multiplicity factor $\mathcal{F}$ (Table VII). This $\mathcal{F}$ factor also incorporates the statistical factor 1/2 if the final state mesons B and C are identical (as illustrated in Fig.6). More details of $\mathcal{F}$ can be found in the Appendix A of Ref.[64]. For $X(1870)$ as the $\eta_2(2^1D_2)$ $n\bar{n}$ meson, the partial decay widths are shown in Table VIII except the channels of $\mathcal{S} + P$ mesons.

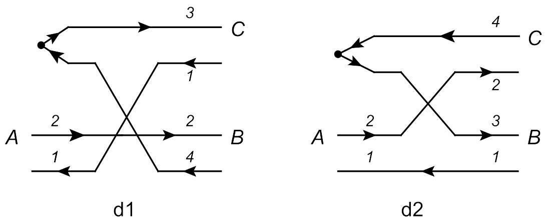

FIG. 6: $q\bar{q}$ meson decay diagrams in the $^3P_0$ decay model.

Decay channels	$\mathcal{I}_{flavor}(d1)$	$\mathcal{I}_{flavor}(d1)$	$\mathcal{F}$
$\rho \to \pi\pi$	$+1/\sqrt{2}$	$-1/\sqrt{2}$	1
$f_2 \to \pi\pi$	$-1/\sqrt{2}$	$-1/\sqrt{2}$	3/2
$f_2 \to KK$	0	$-1/\sqrt{2}$	2
$f_1' \to K^*K$	+1	0	4
$f_2' \to KK$	+1	0	2
$a_2 \to KK$	0	-1	1
$a_2 \to \eta\pi$	+1/2	+1/2	1
$\eta_2 \to \omega\omega$	$-1/\sqrt{2}$	$-1/\sqrt{2}$	1/2
$\eta_2 \to a_i\pi$	$-1/\sqrt{2}$	$-1/\sqrt{2}$	3
$\eta_2 \to f_i\eta$	+1/2	+1/2	1

TABLE VII: Flavor weight factors. Here, $|\eta\rangle = (|n\bar{n}\rangle - |s\bar{s}\rangle)/\sqrt{2}$ and $|\eta'\rangle = (|n\bar{n}\rangle + |s\bar{s}\rangle)/\sqrt{2}$ have been taken for simplicity.

Furthermore, the flux tube model was adopted to check the possibility of $X(1870)$ as a hybrid meson. The partial widths are also listed in Table VIII for the comparison. Details of the flux model are collected in the Appendix B.

Decay	$\eta_2(2^1D_2)$			$\eta_H(0^+0^{-+})$			$f_H(0^+1^{++})$			$\eta_H(0^+2^{-+})$		
channels	Our	Ref. [23]		Our	Ref. [53]		Our	Ref. [53]		Our	Ref. [53]	
K^*K	0.5	17.7	19.3	12.6	10	5	4.9	24.1	18.0	3.2	2.0	1.0
$\rho\rho$	12.9	52.2	56.8	×	×	×	×	×	×	×	×	×
$\omega\omega$	4.2	16.9	18.4	×	×	×	×	×	×	×	×	×
K^*K^*	0.2	2.1	2.3	×	×	×	×	×	×	×	×	×
$a_0(1450)\pi$	16.0	2.4	2.6	56.3	70	175	0.5	×	6	0.5	0.0	0.6
$a_1(1260)\pi$	0.0	15.2	16.6	×	×	×	57.3	14	232	×	0.3	×
$f_1(1280)\eta$	0.0	0.0	0.0	×	×	×	2.5	-	-	×	0.0	×
$a_2(1320)\pi$	54.2	102.5	111.6	8.8	1	16	35.1	5.0	179.4	26.7	25.1	67
$f_2(1275)\eta$	15.1	17.5	19.0	0.0	×	×	1.0	-	-	4.6	0.0	0.0
$\sum\Gamma_i$	103.3	226.5	246.7	77.7	81	196	101.3	43.1	435.4	35.0	27.4	68.6
Expt.	225±14 MeV [1]									$57\pm12^{+19}_{-4}$ MeV [17]		

TABLE VIII: Predictions for the decay width of $X(1870)$ and compared with results from Ref. [23, 53]. A symbol "×" indicates that a decay mode is forbidden. In Ref. [53], the mass of hybrid states is taken as 1.8 GeV.

In Ref. [23], the strength γ is regarded as a free momentum independent constant, and the scale parameter β was taken as

0.4GeV for all mesons. Differently, the momentum dependent creation vertex has been considered here. The effective β (Table I) are adopted in our calculations as that in Ref. [65].

Two groups of the partial widths predicted by the Ref. [53] are quoted in the Table VIII. The left column was given by the flux tube decay model of Isgur, Kokoski, and Paton (IKP) with the "standard parameters" [66]. The right column was by the flux tube decay model of Swanson-Szczepaniak.

As shown in Table VIII, our results do not support $X(1870)$ as the $\eta_2(2^1D_2)$ state since its observed decay width is much smaller than the the theoretical estimate. Furthermore, the BESIII Collaboration claimed that $X(1870)$ primarily decay via $a_0(980)\pi$ [17]. However, $a_2(1320)\pi$ is the largest decay channel in our numerical results and in Ref. [23]. If the partial width of $a_0(980)\pi$ channel is amount to $a_2(1320)\pi$, the width of $X(1870)$ will be much larger than the observed value.

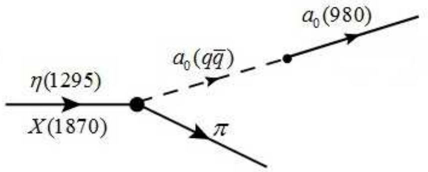

FIG. 7: The diagram for the " $\mathcal{S}$ + P" channels through a virtual intermediate 1^3P_0 $q\bar{q}$ meson.

In the following, we shall evaluate the partial widths of "$\mathcal{S}+P$" channels which have not been given in the tableVIII. As illustrated in the Fig.7, we assume $X(1870)$ decay into $a_0(980)\pi$ via a virtual intermediate 1^3P_0 $q\bar{q}$ meson . We also notice that $\eta(1295)$ dominantly decay into the $\eta\pi\pi$. The three-body decay can occur via three intermediate processes: $\eta(1295) \to \eta\sigma/a_0(980)\pi/\eta(\pi\pi)_{S-wave} \to \eta\pi\pi$[1]. $\eta(1295)$ is proposed to be the first radical excited state of $\eta(550)$. With the ratio $\Gamma(a_0(980)\pi)/\Gamma(\eta\pi\pi) = 0.65 \pm 0.10$ and $\Gamma(\eta(1295)) = 55 \pm 5$MeV, the partial width of $\eta(1295)$ to $a_0(980)\pi$ is estimated no more than 45MeV. The uncertainty of the coupling vertex of $1^3P_0(q\bar{q}) \to a_0(980)$ (see in Fig.7) is assumed to be canceled in the ratio of $\frac{\Gamma(X(1870)\to a_0(980)\pi)}{\Gamma(\eta(1295)\to a_0(980)\pi)}$. The assumption here seems a little rough. However, we just need to evaluate magnitudes of these decay channel.

In our results, the total decay widths of $\Gamma(X(1870) \to \mathcal{S}+P)$ is no more than 12.6MeV and $\Gamma(X(1870) \to a_0(980)\pi) \leq 3.8$MeV. The small decay width of $\Gamma(X(1870) \to a_0(980)\pi)$ also indicates that the $X(1870)$ can't be interpreted as the 2^1D_2 $q\bar{q}$ state.

For a hybrid meson, $X(1870)$ seems most possible to be the $\eta_H(0^+2^{-+})$ state because the total widths exclude the channels of $\mathcal{S}+P$ are much narrow in our work and in Ref.[53]. It is consistent with the width of $X(1870)$.

The assignment for $X(1870)$ as the $f_H(0^+1^{++})$ hybrid seems impossible since the theoretical width is rather broad. But the widths given by the developed flux tube decay model of SS are much small (Table VIII) for the $f_H(0^+1^{++})$ hybrid[53]. So the possibility of $X(1870)$ as a $f_H(0^+1^{++})$ hybrid can not be excluded. We ague that detecting the decay channel of $a_1(1260)\pi$ can pin down this state. Because this channel for the $\eta_H(0^+2^{-+})$ state is forbidden in the flux tube decay model of IKP and very small in the SS flux tube decay model. But it is large enough to be observed for the $f_H(0^+1^{++})$ state in two kinds of flux tube decay model (see in TableVIII).

As shown in Table VIII, $X(1870)$ is impossible to be the $\eta_H(0^+0^{-+})$ hybrid state. The predicted width in both our work and in Ref.[53] are broader. In addition, $\eta\pi$ is a visible channel for both $a_0(1450)$ and $a_2(1320)$. A week signal was found in the region of 1200~1400MeV in the analysis of $\eta\pi^\pm$ (Fig.2(b) of Ref.[17]), which contradicts the large $a_0(1450)\pi$ channel of the $\eta_H(0^+0^{-+})$ state. This also implicates $X(1870)$ disfavor a 0^+0^{-+} hybrid meson.

In our work and the Ref. [23], the channels of $a_2(1320)\pi$ and $f_2(1275)\eta$ are large for the $\eta_2(2^1D_2)$ state, consistent with the observations of the $\eta_2(1870)$. However, the partial widths of K^*K, $\rho\rho$ and $\omega\omega$ in our work are much narrower than the expectations from Ref. [23]. With the mass of 1842 ± 8MeV, the decay width of $\eta_2(1870)$ is predicted about 100MeV which is much lower than the experiments.

If $X(1870)$ and $\eta_2(1870)$ are hybrid and quarkonium states respectively with the 0^+2^{-+} quantum numbers, they should mix with each other. Then the interference enhancement will enlarge the width of $\eta_2(1870)$. The broad decay width of $\eta_2(1870)$ could be explained naturally. On the other hand, $\eta_2(1870)$ has been observed in the channel of $a_0(980)\pi$. However, this channel seems much small if $X(1870)$ is a pure 2^1D_2 $n\bar{n}$ meson. The mixing effect will also enlarge this partial width. Here, we don't plan to discuss $X(1870)$ and $\eta_2(1870)$ further in the mixing scheme for the complex mechanism.

IV. CONCLUSIONS AND DISCUSSIONS

In this work, we analyze the masses and the two-body strong decay of $\eta_2(1870)$ and $X(1870)$. The former listed by PDG is still in dispute. The latter was observed by the BesIII Collaboration recently. Its mass is compatible with $\eta_2(1870)$ but the decay width is much smaller.

Firstly, the average masses, $\overline{M}_{nL}$, are calculated in the the Godfrey-Isgur potential model. The presented $\overline{M}_{nL}$ consist with the experimental data well. According to the results, $X(1870)$ could be the $f_1'(2^3P_1)$, $\eta_2'(1^1D_2)$ and $\eta_2(2^1D_2)$ states. In RTs framework, the possible assignments for $X(1870)$ are the $\eta(3^1S_0)$ and $f_1'(2^3P_1)$ states.

Based on the SU(3) flavor symmetry, we extract the model independent coupling constants for the processes of $f(n\bar{n})/f'(s\bar{s}) \to \mathcal{S}+P$. Then the following conclusions are reached: $a_0\pi$, $\sigma\eta$ and $f_0\eta$ are the dominant channels for $f(n\bar{n})$; κK and $f_0\eta$ are the only decay channels for $f'(s\bar{s})$. For the strong decay properties, both $\eta_2(1870)$ and $X(1870)$ favor a $\eta_2(2^1D_2)$ meson assignment if they are a $n\bar{n}$ meson.

As the $\eta_2(2^1D_2)$ quarkonium, the two-body strong decay of $X(1870)$ is computed in the $^3P_0$ model. The decay width looks much larger than the observation of $X(1870)$. The broad resonance, $\eta_2(1870)$, can be a natural candidate for the 2^1D_2 $n\bar{n}$ meson. There, we fix the creation strength, γ, in two kinds of processes: ①.$n\bar{n} \to n\bar{n} + n\bar{n}$; ②. $n\bar{n} \to n\bar{s} + n\bar{s}$ and $s\bar{s} \to$

$n\bar{s}+n\bar{s}$. The functions of creation vertex are determined as $\gamma(p) = 3.0 + 25\exp(-4p^2)$ and $\gamma(p) = 1.8 + 4\exp(-10p^2)$ respectively.

For the unclear nature of the $\mathcal{S}$ mesons, we just evaluate the magnitude of the partial widths of "$\mathcal{S}+P$" channels by the ratio, $\frac{\Gamma(X(1870)\to a_0(980)\pi)}{\Gamma(\eta(1295)\to a_0(980)\pi)}$, under a rather crude assumption that $\eta(1295)/X(1870) \to a_0(980)\pi$ through a virtual intermediate $1^3P_0\ q\bar{q}$ meson (see Fig.7). The uncertainties of the coupling vertex for $1^3P_0(q\bar{q}) \to a_0(980)$ are assumed to be canceled in the ratio. The total widths of "$\mathcal{S}+P$" are evaluated no more than 7.3MeV. Since $X(1870)$ primarily decay via $a_0(980)\pi$, it also indicated that the $X(1870)$ can't be interpreted as the $2^1D_2\ n\bar{n}$ state.

If $X(1870)$ is a hybrid states, the J^{PC} quantum numbers must be 0^+0^{-+}, 0^+1^{++} and 0^+2^{-+}. Here, we employ the flux model to study the hybrid possibilities. Our results agree well with most of predictions given by Ref. [53]. $X(1870)$ seems most possible to be the $\eta_H(0^+2^{-+})$ state, because the predicted widths are quite narrow, which is consistent with the width of $X(1870)$. But we can't exclude the possibility of 0^+1^{++}. A precise measurement of $a_1(1260)\pi$ and $a_2(1320)\pi$ is suggested to pin down the underlying structure of $X(1870)$.

In addition, the mixture shall occur between $\eta_2(1870)$ and $X(1870)$ when they have the same J^{PC} of 0^+2^{-+}. If the mixing occurs, the interference enhancement should enlarge the width of $\eta_2(1870)$, which can explain the broader decay width of $\eta_2(1870)$ naturally.

In summary, we propose that there are two different isoscalar mesons around 1.8GeV. The broad one, $\eta_2(1870)$, can be interpreted as the $\eta_2(2^1D_2)$ quarkonium. The narrow one, $X(1870)$, looks more like the $\eta_2(0^+2^{-+})$ hybrid meson. The possibility of $X(1870)$ as a $f_H(0^+1^{++})$ hybrid still exists.

Acknowledgments

This project is supported by the National Natural Science Foundation of China (NSFC) under grant No. 11075102 and U1204115, the Innovation Program of Shanghai Municipal Education Commission under grant No. 13ZZ066 and the Program of He'nan Technology Department under grant No. 11147201. It is also supported by the Key Project (Science & Technology) of the He'nan Educational Committee under grant No.13A140014 and the initial scientific research fund for PhD of Anyang Normal University (No.320002).

Appendix A: The expressions of amplitudes

We have omitted a exponential factor in following decay amplitudes $\mathcal{M}_{LS}$ for compactness,

$$\exp(-\frac{2\lambda\mu-\nu^2}{4\mu}p^2). \tag{A1}$$

where we defined

$$\mu=\frac{1}{2}(\frac{1}{\beta_A^2}+\frac{1}{\beta_B^2}+\frac{1}{\beta_C^2});\ \ \nu=\frac{m_1}{(m+m_1)\beta_B^2}+\frac{m_2}{(m+m_2)\beta_C^2}.$$

and

$$\lambda=\frac{m_1^2}{(m+m_1)^2\beta_B^2}+\frac{m_2^2}{(m+m_2)^2\beta_C^2};\quad \eta=\frac{m_1}{m+m_1}.$$

For $1^3S_1 \to 1^1S_0 + 1^1S_0$,

$$\mathcal{M}_{10}=\frac{2\mu-\nu}{8\sqrt{3}\pi^{5/4}\mu^{5/2}(\beta_A\beta_B\beta_C)^{3/2}}p \tag{A2}$$

For $1^3P_2 \to 1^1S_0 + 1^1S_0$,

$$\mathcal{M}_{20}=\frac{2\mu\beta_B^{3/2}-(p^2\nu^2+2\mu(1-p^2\nu))\beta_C^{3/2}}{8\sqrt{15}\pi^{5/4}\mu^{7/2}\beta_A^{5/2}\beta_B^{3/2}\beta_C^3} \tag{A3}$$

For $1^3P_2 \to 1^3S_1 + 1^1S_0$, $\mathcal{M}_{21} = -\sqrt{3/2}\mathcal{M}_{20}$.
For $1^3P_1 \to 1^3S_1 + 1^1S_0$,

$$\mathcal{M}_{01}=\frac{4\mu\beta_B^{3/2}+(p^2\nu^2+2\mu(1-p^2\nu))\beta_C^{3/2}}{24\pi^{5/4}\mu^{7/2}\beta_A^{5/2}\beta_B^{3/2}\beta_C^3} \tag{A4}$$

$$\mathcal{M}_{21}=\frac{(2\mu-\nu)\nu}{24\sqrt{2}\pi^{5/4}\mu^{7/2}\beta_A^{5/2}\beta_B^{3/2}\beta_C^3}p^2 \tag{A5}$$

For $1^3D_3 \to 1^1S_0 + 1^1S_0$,

$$\mathcal{M}_{30}=-\frac{2\mu-\nu}{16\sqrt{35}\pi^{5/4}\mu^{9/2}\beta_A^{7/2}\beta_B^{3/2}\beta_C^{3/2}}\nu^2p^3 \tag{A6}$$

For $2^1S_0 \to 1^3P_0 + 1^1S_0$,

$$\begin{aligned}\mathcal{M}_{11}=&\frac{1}{96\pi^{5/4}\mu^{11/2}\beta_A^{7/2}\beta_B^{5/2}\beta_C^{3/2}}\\ &\times(-24p^2\eta\mu^3-p^4\nu^4+2p^2\mu\nu^2(-10+p^2(1+\eta)\nu)-4\mu^2(15-5p^2(1+\eta)\nu+p^4\eta\nu^2)\\ &+6\mu^2(4p^2\eta\mu^2+p^2\nu^2-2\mu(-3+p^2(1+\eta)\nu))\beta_A^2)\end{aligned} \tag{A7}$$

For $2^1D_2 \to 1^3S_1 + 1^1S_0$,

$$\mathcal{M}_{11}=\frac{-p^4\nu^4+2p^2\nu^2\mu(\nu p^2-14)+28\mu^2(\nu p^2-5)+14\mu^2(p^2\nu^2-2(\nu p^2-5)\mu\beta_A^2)}{160\sqrt{21}\pi^{5/4}\mu^{13/2}\beta_A^{11/2}\beta_B^{3/2}\beta_C^{3/2}}\nu p \tag{A8}$$

$$\mathcal{M}_{31} = \frac{-28\mu^2 + \nu^3 p^2 - 2\mu\nu(\nu p^2 - 9) + 14(2\mu - \nu)\mu^2\beta_A^2}{160\sqrt{14}\pi^{5/4}\mu^{13/2}\beta_A^{11/2}\beta_B^{3/2}\beta_C^{3/2}}\nu^2 p^3 \tag{A9}$$

For $2^1D_2 \to 1^3S_1 + 1^3S_1$, $\mathcal{M}'_{11} = \sqrt{2}\mathcal{M}_{11}$ and $\mathcal{M}'_{31} = \sqrt{2}\mathcal{M}_{31}$.
For $2^1D_2 \to 1^3P_0 + 1^1S_0$

$$\begin{aligned}\mathcal{M}_{20} = & -\frac{1}{192\sqrt{35}\pi^{5/4}\mu^{15/2}\beta_A^{11/2}\beta_B^{5/2}\beta_C^{3/2}} \\ & \times (p^4\nu^5 - 2p^2\mu\nu^3(-18 + p^2(1+\eta)\nu) + 4\mu^2\nu(63 - 11p^2(1+\eta)\nu + p^4\eta\nu^2) + 56\mu^3(-2 + \eta(-2 + p^2\nu)) \\ & - 14\mu^2(p^2\nu^3 - 2\mu\nu(-7 + p^2(1+\eta)\nu) + 4\mu^2(-2 + \eta(-2 + p^2\nu)))\beta_A^2)\nu p^2.\end{aligned} \tag{A10}$$

For $2^1D_2 \to 1^3P_1 + 1^1S_0$

$$\mathcal{M}_{21} = -\frac{p^2\nu^2 - 14\mu^2\beta_A^2 + 14\mu}{16\sqrt{35}\pi^{5/4}\mu^{11/2}\beta_A^{11/2}\beta_B^{5/2}\beta_C^{3/2}}(\eta - 1)\nu p^2. \tag{A11}$$

For $2^1D_2 \to 1^3P_2 + 1^1S_0$

$$\begin{aligned}\mathcal{M}_{02} = & \frac{1}{480\sqrt{14}\pi^{5/4}\mu^{15/2}\beta_A^{11/2}\beta_B^{5/2}\beta_C^{3/2}} \\ & \times (p^6\mu^6 - 2p^4\mu\nu^4(p^2(1+\eta)\nu - 21) + 4p^2\mu^2\nu^2(105 - 14p^2(1+\eta)\nu + p^4\eta\nu^2) + 56\mu^3(15 - 5p^2(1+\eta)\nu \\ & + p^4\eta\nu^2) - 14\mu^2(p^4\nu^4 - 2p^2\mu\nu^2(-10 + p^2(1+\eta)\nu) + 4\mu^2(15 - 5p^2(1+\eta)\nu + p^4\eta\nu^2))\beta_A^2).\end{aligned} \tag{A12}$$

$$\begin{aligned}\mathcal{M}_{22} = & -\frac{1}{672\sqrt{5}\pi^{5/4}\mu^{15/2}\beta_A^{15/2}\beta_B^{5/2}\beta_C^{3/2}} \\ & \times (p^4\nu^5 - 2p^2\mu\nu^3(-18 + p^2(1+\eta)\nu) + 2\mu^2\nu(126 - 25p^2(1+\eta)\nu + 2p^4\eta\nu^2) + 28\mu^3(-7 + \eta(-7 + 2p^2\nu)) \\ & - 14(\mu^2)(p^2\nu^3 - 2\mu\nu(-7 + p^2(1+\eta)\nu) + 2\mu^2(-7 + \eta(-7 + 2p^2\nu)))\beta_A^2)\nu p^2.\end{aligned} \tag{A13}$$

$$\begin{aligned}\mathcal{M}_{42} = & -\frac{1}{1120\pi^{5/4}\mu^{15/2}\beta_A^{11/2}\beta_B^{5/2}\beta_C^{3/2}} \\ & \times (\nu(p^2\nu^3 - 36\mu^2 + 2\mu\nu(11 - p^2\nu)) + 2\eta\mu(28\mu^2 - p^2\nu^3 + 2\mu\nu(p^2\nu - 9)) - 14\mu^2(2\mu - \nu)(2\eta\mu - \nu)\beta_A^2)\nu^2 p^4.\end{aligned} \tag{A14}$$

For $2^1D_2 \to 2^3P_1 + 1^1S_0$

$$\begin{aligned}\mathcal{M}_{21} = & \frac{1}{160\sqrt{14}\pi^{5/4}\mu^{15/2}\beta_A^{11/2}\beta_B^{9/2}\beta_C^{3/2}} \\ & \times (-112\eta\mu^3 + 252\mu^2\nu + 56p^2\eta^2\mu^3\nu - 80p^2\eta\mu^2\nu^2 + 36p^2\mu\nu^3 + 4p^4\eta^2\mu^2\nu^3 - 4p^4\eta\mu\nu^4 + p^4\nu^5 \\ & - 10\mu^2\nu(14\mu + p^2\nu^2)\beta_B^2 - 14\mu^2\beta_A^2(14\mu\nu + 4p^2\eta^2\mu^2\nu + p^2\nu^3 - 4\eta\mu(2\mu + p^2\nu^2) - 10\mu^2\nu\beta_B^2))(\eta - 1)p^2.\end{aligned} \tag{A15}$$

The above amplitudes, $\mathcal{M}_{LS}$, can be reduced further in the approximation of $m_1 = m_2 = m$ and $\beta_A = \beta_B = \beta_C = \beta$. The reduced $\mathcal{M}_{LS}$ are consistent with these given by Ref. [64] except for an unimportant factor, $-2^{9/2}$, since this factor can be absorbed into the coefficient γ.

Appendix B: Hybrid decay in the flux tube model

The flux tube model was motivated by the strong coupling expansion of the lattice QCD. In this model, decay occurs when the flux-tube breaks at any point along its length, with a $q\bar{q}$ pair production in a relative $J^{PC} = 0^{++}$ state. It is similar to the $^3P_0$ decay model but with an essential difference. The flux tube model extend the nonrelativistic constituent quark model to include gluonic degrees of freedom in a very simple and intuitive way, where the gluonic field is regarded as tubes of color flux. Then it can be extended to the hybrid research. When the hybrid mesons are assumed to be narrow, and the threshold effects aren't taken into account, the partial decay width $\Gamma_{LS}(H \to BC)$ is given by the flux model as [67]

$$\Gamma_{LS}(H \to BC) = \frac{p}{(2J_A+1)\pi}\frac{\tilde{M}_B\tilde{M}_C}{\tilde{M}_A}|\mathcal{M}_{LS}(H \to BC)|^2 \quad \text{(B1)}$$

where $\tilde{M}_A$, $\tilde{M}_B$, $\tilde{M}_C$ are the "mock-meson" masses of A, B, C [65]. When a hybrid meson decay into P-wave and pseudoscalar mesons, the partial wave amplitude $\mathcal{M}_L(H \to BC)$ (with $S = S_B$) is given as the following form

$$\mathcal{M}_L(H \to BC) = \langle \phi_B\phi_C|\phi_A\phi_0\rangle\left(\frac{a\tilde{c}}{9\sqrt{3}}\frac{1}{2}A^0_{00}\sqrt{\frac{fb}{\pi}}\right)\frac{\kappa\sqrt{b}}{(1+fb/(2\tilde{\beta}^2))^2}\sqrt{\frac{2\pi}{3\Gamma(3/2+\delta)}}\frac{\beta_A^{3/2+\delta}}{\tilde{\beta}}\tilde{\mathcal{M}}_L(H \to BC) \quad \text{(B2)}$$

B	0^+0^{-+}(H)	0^+1^{++}(H)	0^+2^{-+}(H)
0^{++}	$+\sqrt{2}\mathcal{M}_S/3$	$-\sqrt{2}\mathcal{M}_{P_2}/\sqrt{3}$	$+\mathcal{M}_D/3$
1^{++}	$-$	$-\mathcal{M}_{P_1}/\sqrt{2}$	-
2^{++}	$+\mathcal{M}_D/3$	$-\mathcal{M}_{P_4}/\sqrt{30}$ $+\mathcal{M}_F/\sqrt{5}$	$-\sqrt{5}\mathcal{M}_S/\sqrt{18}$ $-\sqrt{7}\mathcal{M}_D/3$

TABLE IX: Partial wave amplitudes $\tilde{\mathcal{M}}_L(H \to BC)$ for an initial hybrid H decaying into a P-wave and pseudoscalar mesons.

The flavor matrix element $\langle \phi_B\phi_C|\phi_A\phi_0\rangle$ have been discussed before. $\tilde{\mathcal{M}}_L(H \to BC)$ are listed in Table IX for the states of $\eta_H(0^+0^{-+})$, $f_H(0^+1^{++})$ and $\eta_H(0^+2^{-+})$.

Here the $\mathcal{M}_S$, $\mathcal{M}_D$, $\mathcal{M}_{P_i}$ and $\mathcal{M}_F$ are defined as $\mathcal{M}_S = -(3\tilde{h}_0 - \tilde{g}_1 + 4\tilde{h}_2)$, $\mathcal{M}_D = (\tilde{g}_1 + 5\tilde{h}_2)$, $\mathcal{M}_{P_1} = -i(2\tilde{g}_0 + 3\tilde{h}_1 - \tilde{g}_2)$, $\mathcal{M}_{P_2} = -i(\tilde{g}_0 + \tilde{g}_2)$, $\mathcal{M}_{P_4} = -i(10\tilde{g}_0 + 9\tilde{h}_1 + \tilde{g}_2)$ and $\mathcal{M}_F = -3i(\tilde{g}_2 + \tilde{h}_3)$. The analytical expressions of $\tilde{g}_i$ and $\tilde{h}_i$ are given as

$$\tilde{g}_n = 2^{3+\delta}\frac{M^n m}{(M+m)^{n+1}}(2\beta_A^2+\tilde{\beta}^2)^{-\frac{n+\delta+3}{2}}\Gamma\left(\frac{n+\delta+3}{2}\right){}_1F_1\left[\frac{n+\delta+3}{2}, n+1, -\left(\frac{M}{M+m}\right)^2\frac{p^2}{2\beta_A^2+\tilde{\beta}^2}\right]p^{n+1} \quad \text{(B3)}$$

$$\tilde{h}_n = 2^{3+\delta}\tilde{\beta}^2\left(\frac{M}{M+m}\right)^n(2\beta_A^2+\tilde{\beta}^2)^{-\frac{n+\delta+4}{2}}\Gamma\left(\frac{n+\delta+4}{2}\right){}_1F_1\left[\frac{n+\delta+4}{2}, n+1, -\left(\frac{M}{M+m}\right)^2\frac{p^2}{2\beta_A^2+\tilde{\beta}^2}\right]p^n \quad \text{(B4)}$$

where ${}_1F_1[\cdots]$ are the confluent hypergeometric functions. Here we don't take account of the decay channels of $H \to 2S + 1S$ because they are forbidden by the conservation laws, or the "spin selection rule", or the phase space, *e.g.*, the decay channel of $\pi(1300)+\pi$ is forbidden for the $f_H(0^+1^{++})$ state by the "spin selection rule". In this work, we choose to follow the Refs. [67] and take the combination $(a\tilde{c}/9\sqrt{3})\frac{1}{2}A^0_{00}\sqrt{\frac{fb}{\pi}}$ as 0.64 which was fixed by the conventional mesons [65], $M = m = m_{u,d} = 330$MeV, $\tilde{M}_B^{I=0} = \tilde{M}_B^{I=1} = 1250$MeV, $\tilde{M}_C^{I=0} = 720$MeV, $\tilde{M}_C^{I=1} = 850$MeV, $\beta_A = 0.27$GeV, $\delta = 0.62$, $b = 0.18\text{GeV}^2$ and $\kappa = 0.9$. Final states containing π have $\tilde{\beta} = 0.36$GeV, otherwise $\tilde{\beta} = 0.40$GeV.

[1] J. Beringer *et al.* (Particle Data Group), Phys. Rev. D **86**, 010001 (2012).

[2] C.A. Meyer and Y. Van Haarlem, Phys. Rev. C **82**, 025208 (2010).

[3] B. Aubert *et al.* (BABAR Collaboration), Phys. Rev. D **76**, 012008 (2007).

[4] J. P. Lees *et al.* (BABAR Collaboration), Phys. Rev. D **86**, 012008 (2012).

[5] M. Ablikim *et al.* (BES Collaboration), Phys. Rev. Lett. **100**, 102003 (2008).

[6] C. P. Shen *et al.* (Belle Collaboration), Phys. Rev. D **80**, 031101(R) (2009).

[7] Gui-Jun Ding and Mu-lin Yan, Phys. Lett. B **650**, 390 (2007).

[8] Gui-Jun Ding and Mu-lin Yan, Phys. Lett. B **657**, 49 (2007).

[9] Zhi-Gang Wang, Nucl. Phys. **A791**, 106 (2007).

[10] Hua-Xing Chen, Xiang Liu, A. Hosaka and Shi-Lin Zhu, Phys. Rev. D **78**, 034012 (2008).

[11] Shi-Lin Zhu, Int.J.Mod.Phys.E **17**, 283, (2008).

[12] K. Karch *et al*. (Crystall Ball Collaboration), Phys. Lett. B **249**, 583 (1990).

[13] M. Feindt, DESY-90-128 (1990).

[14] J.Z. Bai *et al*. (BES Collaboration), Phys. Lett. B **446**, 356 (1999).

[15] J. Adomeit *et al*. (Crystal Barrel Collaboration), Z. Phys. C **71**, 227 (1996).

[16] A.V. Anisovich *et al*., Phys. Lett. B **477**, 19 (2000).

[17] M. Ablikim *et al*. (BES Collaboration), Phys. Rev. Lett. **107**, 182001 (2011).

[18] M.S. Chanowitz and S.R. Sharpe, Nucl. Phys. **B222**, 211 (1983).

[19] T. Barnes, F. Close and F. de Viron, Nucl. Phys. **B224**, 241 (1983).

[20] N. Isgur and J.E. Paton, Phys. Rev. D **31**, 2910 (1985).

[21] T. Barnes, F.E. Close and E.S. Swanson, Phys. Rev. D **52**, 5242 (1995).

[22] S. Ishida, H. Sawazaki, M. Oda and K. Yamada, Phys. Rev. D **47**, 179 (1993).

[23] De-Min Li and En Wang, Eur. Phys. J. C **63**, 297 (2009).

[24] S. Godfrey and N. Isgur, Phys. Rev. D **32**, 189 (1985).

[25] E. Eichten, K. Gottfried, T. Kinoshita, J.B. Kogut, K.D. Lane and T.M. Yan, Phys. Rev. Lett. **34**, 369 (1975).

[26] E.E. Salpeter and H.A.Bethe, Phys. Rev. **84**, 1232 (1951).

[27] E.E. Salpeter, Phys. Rev. **87**, 328 (1952).

[28] D.S. Hwang, C.S. Kim and W. Namgung, Z. Phys. C 69, 107 (1995).

[29] S.F. Radford, W.W. Repko and M.J. Saelim, Phys. Rev. D **80**, 034012 (2009).

[30] S.F. Radford and W.W. Repko, Phys. Rev. D **75**, 074031 (2007).

[31] W. Roberts and B. Silvestre-Brac, Phys. Rev. D **57**, 1694 (1998).

[32] T. Barnes, S. Godfrey and E.S. Swanson, Phys. Rev. D **72**, 054026 (2005).

[33] A.M. Badalian and B.L.G. Bakker, Phys. Rev. D **64**, 114010 (2001).

[34] A.M. Badalian, B.L.G. Bakker and Yu.A. Simonov, Phys. Rev. D **66**, 034026 (2002).

[35] P. González, Phys. Rev. D **80**, 054010 (2009).

[36] S. Godfrey and R. Kokoski, Phys. Rev. D **43**, 1679 (1991).

[37] F.E. Close and E.S. Swanson, Phys. Rev. D **72**, 094004 (2005).

[38] De-Min Li, Peng-Fei Ji and Bing Ma, Eur. Phys. J. C **71**, 1582 (2011).

[39] D. Ebert, R.N. Faustov and V.O. Galkin, Phys. Rev. D **79**, 114029 (2009).

[40] R. Giachetti and E. Sorace, Phys. Rev. D **87**, 034021 (2013).

[41] P. Masjuan, E.R. Arriola and W. Broniowski, Phys. Rev. D **85**, 094006 (2012).

[42] L. Maiani, F. Piccinini, A.D. Polosa and V. Riquer, Phys. Rev. Lett. **93**, 212002 (2004).

[43] J.D. Weinstein and N. Isgur, Phys. Rev. Lett. 48 , 659 (1982); Phys. Rev. D **27**, 588 (1983); Phys. Rev. D **41**, 2236 (1990).

[44] R.L. Jaffe, Phys. Rev. D **15**, 281 (1977); R.L. Jaffe and F.E. Low, Phys. Rev .D **19**, 2105 (1979); M. Alford and R.L. Jaffe, Nucl. Phys. **B578**, 367 (2000).

[45] Zhi-Gang Luo, Xiao-Lin Chen and Xiang Liu, Phys. Rev . D **79**, 074020 (2009).

[46] Jie-Sheng Yu, Zhi-Feng Sun, Xiang Liu and Qiang Zhao, Phys. Rev. D **83**, 114007 (2011).

[47] Jia-Feng Liu, Gui-Jun Ding and Mu-Lin Yan, Phys. Rev. D **82**, 074026 (2010).

[48] R.L. Jaffe, Phys. Rept. **409**, 1 (2005).

[49] A. Selem and F. Wilczek, hep-ph/0602128.

[50] E. Santopinto and G. Galatà, Phys. Rev. C **75**, 045206 (2007).

[51] J.J. de Swart, Rev. Mod. Phys. **35**. 916 (1963).

[52] C. Amsler and F.E. Close, Phys. Rev.D **53**, 295 (1996).

[53] P.R. Page, E.S. Swanson and A.P. Szczepaniak, Phys. Rev. D **59**, 034016 (1999).

[54] L. Micu, Nucl. Phys. **B10**, 521 (1969).

[55] A. Le Yaouanc, L. Olivier, O. Pene, and J.C. Raynal, Phys. Rev. D **8**, 2223 (1973); A. Le Yaouanc, L. Oliver, O. Pene, and J.C. Raynal, *Hadron Transition in the Quark Model*(Gordon and Breach, New York, 1988), p. 311.

[56] Zao-Chen Ye, Xiao Wang, Xiang Liu and Qiang Zhao, Phys. Rev. D **86**, 054025 (2012).

[57] C. Hayne and N. Isgur, Phys. Rev. D **25**, 1944 (1982).

[58] M. Jacob and G.C. Wick, Ann. Phys. (N.Y.) **7**, 404 (1959).

[59] P. Geiger and E.S. Swanson, Phys. Rev. D **50**, 6855 (1994).

[60] H.G. Blundel, arXiv:hep-ph/9608473.

[61] R. Bonnaz and B. Silvestre-Brac, Few-Body Syst. **27**, 163 (1999).

[62] E.S. Ackleh, T. Barnes and E.S. Swanson, Phys. Rev. D **54**, 6811 (1996).

[63] J. Segovia, D.R. Entem and F. Fernandez, Phys. Lett. B **715**, 322 (2012).

[64] T. Barnes, F.E. Close, P.R. Page and E.S. Swanson, Phys. Rev. D **55**, 4157 (1997).

[65] R. Kokoski and N. Isgur, Phys. Rev. D **35**, 907 (1987).

[66] N. Isgur, R. Kokoski, and J. Paton, Phys. Rev. Lett. **54**, 869 (1985).

[67] F.E. Close, P.R. Page, Nucl. Phys. **B443**, 223, (1995).